IJTMGH International Journal of Travel Medicine and Global Health

Int J Travel Med Glob Health. 2024 Jun;12(2):90-109 doi 10.30491/IJTMGH.2023.431376.1395
http://ijtmgh.com

Original Article Open Access

Evaluation of apparent diffusion coefficient values in discriminating concurrent differential diagnosis of Glioblastoma, lymphoma, and metastatic tumors

Mersad Mehrnahad[1]*, Morteza Sanei Taheri[2], Farnaz Kimia[1], Hamidreza Saligheh Rad[3], Robabeh Ghodssi GhassemAbadi[4]

[1] Department of Radiology, Qom University of Medical Sciences, Qom, Iran
[2] Department of Radiology, Shahid Beheshti University of Medical Sciences, Tehran, Iran
[3] Quantitative MR Imaging and Spectroscopy Group (QMISG), Research Center for Molecular and Cellular Imaging, Tehran University of Medical Sciences, Tehran, Iran
[4] Department of Biostatistics, Faculty of Medical Sciences, Tarbiat Modares University, Tehran, Iran

***Corresponding Author:** Department of Radiology, Qom University of Medical Sciences, Qom, Iran. Email: mersad.mehr@googlemail.com, Phone: 09126070465.

Received 2023-12-19; **Accepted** 2023-12-31; **Online Published** 2024-06-01

Abstract

Background: Apparent diffusion coefficient (ADC) statistics can be valuable in distinguishing three types of brain tumors. The aim is to evaluate the capability of volume under the receiver operating characteristic (ROC) surface (VUS) for concurrent differential diagnosis of glioblastoma (GBM), lymphoma (LYM), and metastatic tumor(s) (MTTs) lesions of brain malignancies.

Methods: Investigated Magnetic Resonance Imaging (MRI) included 57 GBM, 25 LYM, and 25 MTT that were pathological diagnoses, after MR imaging. Region of interest (ROI) was taken from tumor regions (TUMOR), enhancement area (ENHANCED), and peritumoral edema (EDEM) regions. ADC maps were obtained after selecting a region of interest, and First-Order Histogram Features (FOHs) were extracted. Statistical analysis was performed by MedCalc version 15.8 for comparison of continuous variables between three groups of lesions and plotting the ROC curves. For VUS and correct classification rates (CCR) calculations the R software v2.13.1 with the DiagTest3grp package was used. The confidence interval level was 95% for significant results. Diagnostic accuracy of ADC in the differentiation of mentioned three groups was performed using ROC surface.

Results: ADC_{Min}, ADC_{75} and $ADC_{95\ Percentile}$ values in TUMOR groups of ROI, $ADC_{Maximum}$, ADC_{Min}, ADC_{Mean}, ADC_{Median} , $ADC_{Uniformity}$ and $ADC_{Entropy}$ in ENHANCED and ADC_{25}, ADC_{75}, $ADC_{95\ Percentiles}$, ADC_{Mean} , $ADC_{Normal\ Mean}$, ADC_{Median}, $ADC_{Entropy}$, $ADC_{Third\ Moment}$ and $ADC_{StandardDeviation}$ in EDEM had significant VUS values results among GBM, LYM and MTTs .

Conclusion: VUS analysis is a helpful statistical method for categorizing types of brain tumors. Using the application of FOHs and proposed cut-off points for them by the VUS analysis, the differentiation of more than two types of brain tumors would be possible, concurrently. This will help neurologists and neurosurgeons to plan their treatment and surgery or monitor the status of patients' therapeutic needs.

Keywords: Apparent diffusion coefficient, glioblastoma, lymphoma, Magnetic resonance Imaging, ROC surface (VUS).

Citation: Mehrnahad M, Taheri MS, Kimia F, Saligheh Rad H , Ghodssi R Abadi Gh. Evaluation of apparent diffusion coefficient values in discriminating concurrent differential diagnosis of Glioblastoma, lymphoma, and metastatic tumors. Int J Travel Med Glob Health, 2024;12(2):90-109. doi: 10.30491/IJTMGH.2023.431376.1395

Introduction

ADC can be calculated from MRI-based methods and it can be applied as biomarkers in differential diagnosis and grading of brain tumors, or even monitoring the therapy[1-3]. This biomarker provides early diagnosis, selecting treatment strategy, and expenditures of the therapeutic or other diagnostic methods [4]. GBM is of the most prevalent brain tumors with a poor prognosis; the five-year survival rate of GBM is estimated to be less than 5% [5]. Despite GBM, central nervous system (CNS) lymphoma is a rare malignancy with a better prognosis [6, 7].

MRI-based diagnostic methods are used for the diagnosis of GBM, lymphoma, and metastatic lesions [4, 8-10]. However, distinguishing primary brain tumors,

metastatic lesions, and lymphomas is difficult and critical for surgical or therapeutic interventions [11].

New biomarkers for diagnostic radiology mainly depend on statistics and image analysis of MRIs with or without enhancement [12-14]. Biomarker-exploring investigations mainly rely on comparative statistics and receiver operating characteristic (ROC) analysis. However, the usability of the other statistical facilities, such as volume under the ROC surface (VUS) has been less mentioned in neuroradiology. VUS analysis is applicable when more than two, mostly three, categories of conditions should be diagnosed differentially. In this situation, two cut-off points will be calculated for three categories whereas in conventional ROC analysis only one cut-off is obtained to differentiate two groups. [15, 16]. As many disease conditions have more than two types of categories or classes the VUS analysis would be of worth for clinicians, especially when making diagnoses and decisions. This analysis method is useful in predicting the types of brain malignancies when exploring MRIs.

VUS analysis helps scientists to obtain two useful cut-off points for concurrent differentiation of three types of the malignant brain in addition to the calculation of CCR. Correct classification rate helps determine the best cut-offs and highest correct classification rate when distinguishing more than two variables using VUS or three-way ROC plots [15]. This study aimed to investigate three types of ROI, including tumor and an enhanced area along with peritumoral edema of the lesions, concurrently. The FOHs of ADC map the concurrent differential diagnosis of GBM, brain LYM, and MTT was assessed.

Material and methods

Study ethics

This work is done by the radiology department of Shohaday-e-Tajrish hospital in Tehran city, the capital of Iran. MRI data and pathological results of tumor types were gathered only from patients who or their guardians declared their favorites to be included in the study. All patients were under the routine protocol of diagnosis and interventions; then, no additional diagnostic or operative acts were done on the patients. The study population was patients who were referred to university hospitals from April 2018 to April 2019. The proposal was approved by the ethical committee of Shahid Beheshti University of Medical Sciences.

Classification of MRIs according to the surgical pathology results

MR imaging was done before surgical operation and pathology diagnosis. After primary diagnosis with the MRI, the neurosurgery was done on each patient for treatment and diagnostic purposes, according to the therapeutic protocols. Then, we have only included the MRIs of those patients with the surgical pathology results. The pathological method was the routine method. Briefly, the dissected brain lesions were fixed with formalin following tissue processing. Paraffin-embedding was done and followed by tissue sectioning using a microtome. A standard method of hematoxylin and eosin (H&E) method was performed. Prepared slides were explored by a highly-experienced and sophisticated pathologist. All MRI data were belonging to that pathological diagnosis included glioblastomas (GBM), brain lymphomas (LYM), and metastatic tumors (MTT).

Image Acquisition

MR imaging was performed on a 1.5 Tesla scanner (Siemens®, Avanto, Rel 16.0). The protocol for tumor MRI included pre-and post-contrast axial and sagittal spin-echo T1-weighted images (TR/TE= 400/12 ms, axial and coronal spin-echo T2 weighted images (TR/TE= 3600/97 ms), axial fluid-attenuated inversion recovery images (TR/TE= 4000/117 msAxial diffusion-weighted imaging was performed using an echo-planar sequence with b-values of 0 and 1000 s/mm2 in three orthogonal directions. ADC maps between b-values of 0 and 1000 were generated on the scanner console. Contrast-enhanced images were taken after intravenous administration of 0.1 mmole/Kg gadopentetate dimeglumine.

MRI analysis and extracting the first order histogram features (FOH)

Three types of ROIs were manually delineated on anatomical images by a junior radiologist (M.M with 4yr of experience) under supervision of and in consensus with a senior radiologist (M. S. with 20yr of experience in neuro-radiology): (1) tumor borders on FLAIR images (the hemorrhagic and necrotic area was avoided); (2) peritumoral edema on FLAIR images; and (3) enhancement area, representing borders of the enhanced regions on post-contrast T1-weighted images. The ROIs were selected using ImageJ software (http://rsb.info.nih.gov/ij/) on the whole image volume encompassing the pathogenic areas.

ADC-maps were co-registered to their corresponding post-contrast axial T1- and FLAIR images using a rigid-body intra-subject registration approach with normalize mutual information (NMI) similarity measure and trilinear transformation method (FMRIB's Linear Image Registration Tool (FLIRT), FSL Library, https://fsl.fmrib.ox.ac.uk/fsl/fslwiki).

First-order histogram (FOH) features, including mean, maximum, minimum, Median, Normal Mean, Standard deviation, Smoothness, Third moment, Uniformity, Entropy, Kurtosis, 25^{th} , 75^{th} and 95^{th} Percentiles, were calculated from the distribution of ADC-values within each of the ROIs. Control ADC values were calculated

from normal-appearing contralateral white matter by mirroring the pathogenic ROIs.

Statistical analysis

The normal distribution of FOH features was assessed by the Shapiro-Wilk test. Mean differences were assessed by ANOVA or Kruskal-Wallis test followed by posthoc tests whenever it was necessary. The diagnostic performance of FOH features in distinguishing MTT, LYM, and GBM was assessed by calculating VUS and its 95% confidence interval. VUS is calculated based on three CCR obtained from each category. As AUC the ideal VUS is obtained where three CCR reach their maximum values. A diagnostic test is considered "poor" where the VUS is close to 0.17 (no more than chance) and "good" when it approaches unity [16, 17]. The bootstrap method was applied for the calculation of the confidence interval of VUS for the non-normal distributed variable. Best cut-off points were determined according to the maximum correct classification rate (CCR) of each category. Area under the ROC Curve (AUC) was calculated for each variable as a post-hoc for VUS. We used the DiagTest3grp package in R software v2.13.1 to calculate VUS. P values less than 0.05 were considered significant. The MedCalc version 15.8 (MedCalc Software bvba, Ostend, Belgium; https://www.medcalc.org; 2015) was used for statistical analysis. Meaningful results were assessed using Kruskal-Wallis and the confidence interval equal to 95% was considered. Further, for VUS and correct classification rates (CCR) calculations we used the R software v2.13.1 with the DiagTest3grp package. VUS is calculated according to the CCR and was used to determine the predictive value of each FOH feature in the categories GBM, LYM, and MTT. The values of VUS lesser than 0.17 are considered weak and the values nearest to 1 are considered as powerful. We used the nonparametric bootstrap method for VUS calculation. In addition, ROC curves were plotted for FOH features in the TUMOR, ENHANCED, and EDEM groups to evaluate the potency of FOHs for differential diagnosis between GBM, Lymphoma, and metastasis.

Results

FOH features among GBM, LYM, and MTT groups showed that Mean, Maximum, Median, Smoothness, Uniformity, Kurtosis, 75, and 95 Percentiles were meaningfully different (P<0.05) (Table 1).

Table 1. Comparison of First-order histogram features (FOHs), extracted from Tumor region, among GBM, Lymphoma, and Metastasis groups.

	GBM (N=57)		Lymph (N=25)		Metastasis (N=25)		P-value
	Mean±SD	Median (min , max)	Mean±SD	Median (min , max)	Mean±SD	Median (min , max)	
Mean	1.287±0.406	1.201* (0.111,2.554)	1.045±0.208	1.025 (0.699,1.420)	1.229±0.428	1.136 (0.671,2.502)	0.014
Maximum	2.273±0.696	2.153* (0.228,3.794)	1.942±0.320	1.979 (1.247,2.510)	2.049±0.547	1.834 (1.383,3.561)	0.043
Minimum	0.635±0.228	0.614 (0.078,1.407)	0.571±0.117	0.582 (0.344,0.771)	0.557±0.215	0.604 (0.143,0.979)	0.188
Median	1.249±0.421	1.168* (0.107,2.603)	1.014±0.225	0.975 (0.656,1.404)	1.214±0.462	1.133 (0.645,2.578)	0.026
Normal Mean	0.563±0.096	0.552 (0.359,0.777)	0.531±0.082	0.542 (0.361,0.649)	0.587±0.104	0.594 (0.330,0.762)	0.105
Standard deviation	0.127±0.033	0.123 (0.076,0.217)	0.124±0.021	0.124 (0.082,0.183)	0.141±0.035	0.130 (0.097,0.220)	0.182
Third moment	0.001±0.002	0.001 (-0.003,0.009)	0.002±0.001	0.002 (-0.001,0.004)	0.001±0.002	0.001 (-0.004,0.003)	0.34
Uniformity	1459.8±1089.6	1245.6‡ (185.4,4386.7)	1135±1051.2	829.9 (87.68,4755)	784.1±612.3	687.3 (51.22,2241)	0.012
Entropy	6.695±0.331	6.699 (6.002,7.461)	6.667±0.291	6.713 (6.026,7.295)	6.736±0.274	6.745 (6.260,7.257)	0.714
Kurtosis	4.176±2.201	3.361 (1.924,10.946)	4.443±2.123	3.636 (2.109,9.299)	3.620±2.055	2.942 (1.751,11.88)	0.08
25 Percentile	0.471±. 0.106	0.462 (0.231,0.719)	0.440±0.074	0.459 (0.290,0.533)	0.483±0.109	0.474 (0.264,0.662)	0.28
75 Percentile	0.643±0.106	0.648 (0.433,0.849)	0.604±0.102£	0.612 (0.391,0.772)	0.683±0.121	0.689 (0.371,0.906)	0.033
95 Percentile	0.792±0.088	0.807 (0.574,0.936)	0.759±0.095£	0.788 (0.565,0.899)	0.826±0.111	0.857 (0.499,0.946)	0.046

* P-value< 0.05 compared with Metastatic group. ‡ P-value< 0.05 compared with Lymph group. £ P-value< 0.05 compared with Metastatic group.

The FOHs were obtained from contrast-enhanced MRIs in GBM, LYM, and MTT groups. Mean, Maximum, Median, Standard deviation, Smoothness, Uniformity, and Entropy was statistically significant among groups (CI= 95%; P<0.05) (Table 2).

Table 2. Comparison of First-order histogram features (FOHs), extracted from Contrast-Enhanced regions, among GBM, Lymphoma, and Metastasis.

	GBM (N=57)		Lymph (N=25)		Metastasis (N=25)		P-value
	Mean±SD	Median (min , max)	Mean±SD	Median (min , max)	Mean±SD	Median (min , max)	
Mean	1.285±0.391	1.244*‡ (0.112,2.318)	0.954±0.136	0.986 (0.703,1.151)	1.104±0.332	0.970 (0.658,2.020)	<0.001
Maximum	2.236±0.615*	2.204 (0.256,3.784)	1.693±0.267	1.687 (1.132,2.291)	1.918±0.467	1.784 (1.292,2.799)	<0.001
Minimum	0.656±0.227	0.671 (0.080,1.592)	0.601±0.113	0.632 (0.342,0.737)	0.537±0.209	0.524 (0.185,0.961)	0.084
Median	1.262±0.426	1.188*‡ (0.106,2.412)	0.915±0.139	0.939 (0.669,1.129)	1.067±0.347	0.940 (0.581,2.033)	<0.001
Normal Mean	0.568±0.107	0.571 (0.382,0.888)	0.567±0.099	0.578 (0.373,0.813)	0.570±0.086	0.584 (0.389,0.732)	0.996
Standard deviation	0.121±0.031	0.115‡ (0.074,0.225)	0.118±0.024	0.112£ (0.079,0.171)	0.140±0.031	0.129 (0.085,0.195we)	0.026
Third moment	0.001±0.003	0.001 (-0.006,0.015)	0.002±0.001	0.002 (1.3E-4,0.006)	0.002±0.002	0.001 (-0.002,0.007)	0.463
Uniformity	499.7±387.9	387.9*‡ (408.9,37.25)	236.7±172.0	223.9 (41.54,731.9)	219.7±201.5	181.7 (22.69,1007.9)	<0.001
Entropy	6.520±0.414	6.593* (4.888,7.342)	6.308±0.301	6.351£ (5.732,6.949)	6.559 ±0.367	6.548 (5.397, 7.139)	0.006
Kurtosis	4.777±2.705	3.802 (2.084,13.52)	4.821±2.123	4.279 (2.545,9.870)	3.666±1.518	3.205 (2.089,8.432)	0.064
25 Percentile	0.483±. 0.113	0.476 (0.203,0.836)	0.484±0.105	0.493 (0.306,0.763)	0.470±0.092	0.491 (0.305,0.684)	0.885
75 Percentile	0.638±0.118	0.635 (0.411,0.959)	0.630±0.105	0.644 (0.417,0.861)	0.660±0.098	0.678 (0.433,0.824)	0.65
95 Percentile	0.787±0.097	0.809 (0.565,0.993)	0.793±0.095	0.814 (0.548,0.957)	0.822±0.081	0.838 (0.622,0.921)	0.347

* P-value< 0.05 compared with Metastatic group. ‡ P-value< 0.05 compared with Lymph group. £ P-value< 0.05 compared with Metastatic group.

The FOHs were obtained from peritumoral edematous regions MRIs in GBM, LYM, and MTT groups. Mean, Minimum, Median, Normal Mean, Standard deviation, Third moment, Entropy, 25, 75, and 95 Percentiles are meaningfully different between groups (CI= 95%; P<0.05) (Table 3).

Table 3. Comparison of first-order histogram features (FOHs), extracted from peritumoral edematous region MRIs, among GBM, and Lymphoma

	GBM (N=57)		Lymph (N=25)		Metastasis (N=25)		P-value
	Mean±SD	Median (min , max)	Mean±SD	Median (min , max)	Mean±SD	Median (min , max)	
Mean	1.416±0.316	1.454‡ (0.125,2.076)	1.184±0.204	1.157£ (0.839,1.525)	1.409±0.358	1.346 (0.887,2.365)	0.002
Maximum	2.020±0.560	2.060 (0.169,3.581)	2.007±0.269	2.050 (1.421,2.461)	2.150±0.482	1.994 (1.621,3.561)	0.981
Minimum	0.739±0.247	0.815*‡ (0.079,1.062)	0.612±0.167	0.556 (0.360,1.024)	0.601±0.179	0.629 (0.263,0.979)	0.014
Median	1.423±0.324	1.474‡ (0.125,2.107)	1.168±0.236	1.139£ (0.759,1.547)	1.425±0.395	1.383 (0.824,2.514)	0.003
Normal Mean	0.704±0.106	0.736*‡ (0.364,0.841)	0.584±0.098	0.586£ (0.403,0.757)	0.650±0.102	0.678 (0.397,0.755)	<0.001
Standard deviation	0.105±0.021	0.102*‡ (0.069,0.159)	0.122±0.019	0.124£ (0.082,0.162)	0.139±0.028	0.133 (0.108,0.216)	<0.001
Third moment	-0.0002±0.002	-1E-4‡ (-0.007,0.007)	0.0008±0.001	0.0007£ (-0.001,0.004)	-5.09E-4±0.002	-7.46E-4 (-0.006,0.003)	0.01
Uniformity	2211.6±1278.6	2168.4 (270.4,5593.4)	2084.6±1466.2	1562.01 (554.7,5341.5)	2031.3±1368.5	1990.4 (221.8,4602.6)	0.847
Entropy	6.564±0.231	6.528‡ (6.115,6.971)	6.752±0.201	6.784 (6.260,7.066)	6.801±0.191	6.813 (6.312,7.178)	0.001
Kurtosis	3.531±1.066	3.243 (2.291,6.949)	3.510±1.333	3.058 (2.192,7.679)	3.420±1.427	2.840 (2.119,9.031)	0.484
25 Percentile	0.639±. 0.119	0.681‡ (0.254,0.797)	0.492±0.103	0.498 (0.334,0.675)	0.555±0.106	0.588 (0.288,0.682)	<0.001
75 Percentile	0.775±0.106	0.806‡ (0.428,0.901)	0.666±0.104	0.661£ (0.450,0.831)	0.750±0.118	0.798 (0.426,0.891)	0.002
95 Percentile	0.868± 0.074	0.882‡ (0.694,0.950)	0.795± 0.090	0.799£ (0.566,0.929)	0.861±0.087	0.895 (0.621,0.950)	0.005

Table 4 presented the volume under the ROC surface (VUS), two cut-off points, the order of categories, and three correct classification rates (CCR1, CCR2, and CCR3) percent of 5categories. The column of ordered categories represents the order of CCR1, CCR2, and CCR3 according to the cut-offs 1 and 2 (next right columns). The VUS values were almost not so powerful for differential diagnosis of metastatic tumors from GBM and LYM malignancies. The most potent value in this table relates to the 95 Percentile; the VUS= 0.292 (95%CI: 0.186-0.397) with cut-off values equal to 0.7968 and 0.8491 discriminate and representative of MTT from LYM and GBM, with the correct classification rates of 64%, 29.8% and 57.1% of cases, respectively. **Figure 1**, represents the VUS scatter-plot and box-plots of each FOH feature for the Tumor ROI; these plots show a better view of data scattering, comparisons of group's mean, and the overlaps of data.

Table 4. VUS values and related cut-off points for each FOH feature extracted from Tumor regions MRIs.

FOH features	VUS (95% CI)	Ordered Categories	Cut 1	Cut 2	CCR_1%	CCR_2%	CCR_3%
Mean	0.265 (0.164,0.377)	LMG	0.9426	1.1621	44	35.7	64.9
Maximum	0.215 (0.125,0.310)	LMG	1.4473	1.8862	12	50	73.7
Minimum	0.279 (0.184,0.373)	MLG	0.5225	0.5972	46.4	40	57.9
Median	0.267 (0.160,0.376)	LMG	0.923	1.148	44	35.7	57.9
Normal Mean	0.260 (0.162,0.358)	LGM	0.4288	0.6084	20	66.7	50
Standard deviation	0.199 (0.122,0.287)	LGM	0.1275	0.1702	72	31.6	28.6
Third moment	0.218 (0.128,0.340)	MGL	0.0002	0.0012	28.6	47.4	64
Uniformity	0.273 (0.168,0.362)	MLG	217.8433	997.2695	28.6	56	59.7
Entropy	0.186 (0.103,0.268)	LGM	6.7796	7..0282	76	29.8	21.4
Kurtosis	0.261 (0.169,0.374)	MGL	2.8429	3.9118	50	36.8	48
25 Percentile	0.223 (0.133,0.313)	LGM	0.4606	0.5076	56	24.6	46.4
75 Percentile	0.290 (0.186,0.393)	LGM	0.6307	0.7519	60	36.8	35.7
95 Percentile	0.292 (0.186,0.397)	LMG	0.7968	0.8491	64	29.8	57.1

Abbreviations: L, Lymphoma; G, GBM; M, Metastatic; VUS, Volume Under the ROC Surface.

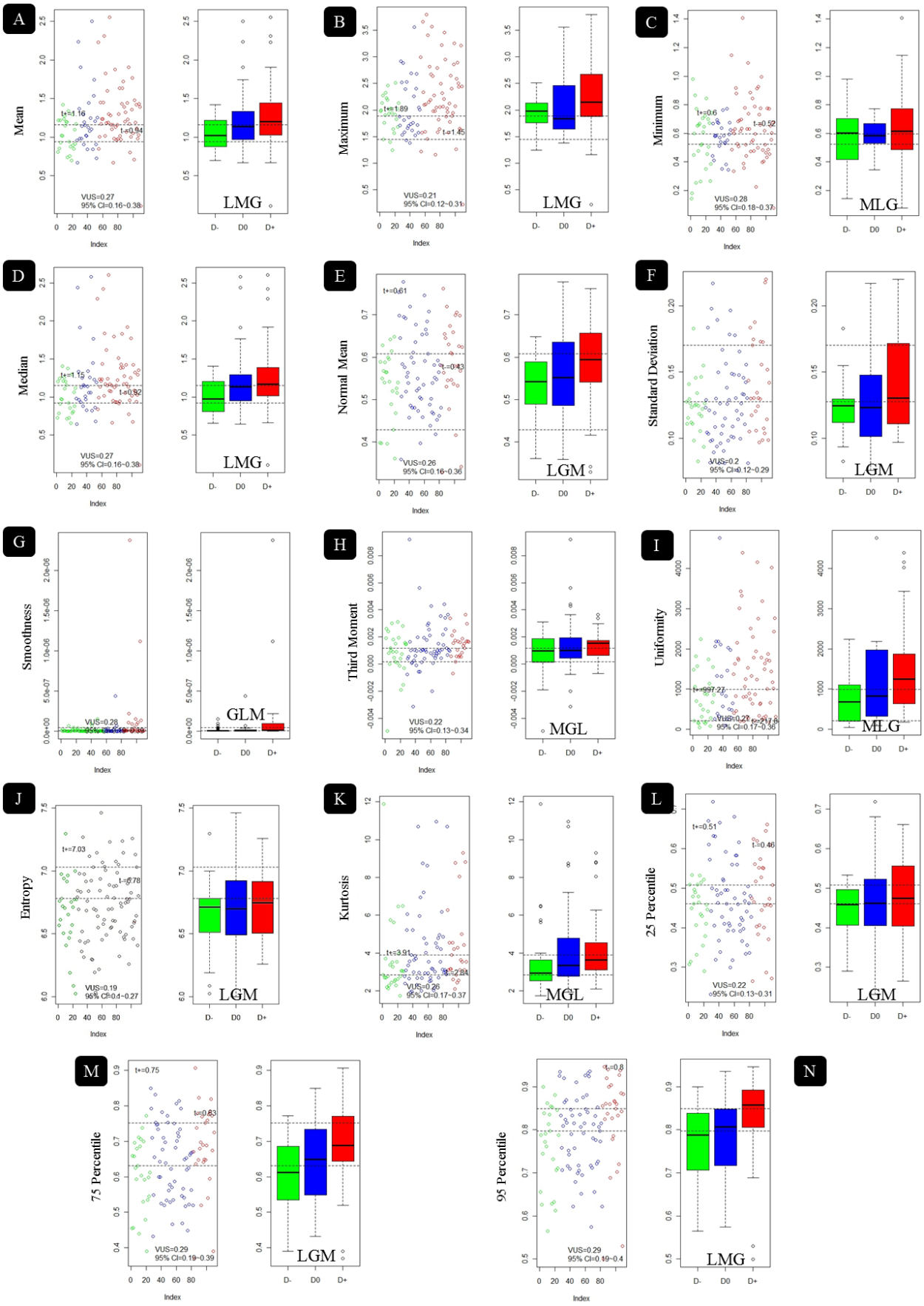

Figure 1. VUS of FOH features in Tumor group (Flair MRIs); the box-plots and scatter-plots show the comparison of three investigated groups (in three-dimensional ROC). The order of plots is according to column 3 of Table 4; the order is shown in box-plot histograms.

Table 5 showed the VUS values for the MRIs taken by contrast-enhancing material. The best VUS value was obtained for ADC-maximum with the VUS= 0.358 (0.254, 0.492) and cut-off equal to 1.7074 and 2.0178; these cut-offs together distinguish the LYM, MTT, and GBM with the rates of correct classification equal to 65%, 38.1%, and 66%. However, other potent VUS include ADC-Median, Uniformity, Minimum, Mean, and Entropy (Table 5). Again, all VUSs presented in Table 5, estimated to be potent in the differential diagnosis of brain lesions including GBM, LYM, and MTT when MRIs took after gadopentetate dimeglumine administration. Figure 2, represented the VUS scatter-plot and box-plots of each FOH feature for the contrast-enhanced MRIs.

Table 5. VUS values and related cut-off points for each FOH feature extracted from Contrast-Enhanced MRIs category.

FOH features	VUS (95% CI)	Ordered Categories	Cut 1	Cut 2	CCR_1%	CCR_2%	CCR_3%
Mean	0.322 (0.211,0.451)	LMG	0.8292	1.0922	30	57.1	74
Maximum	0.358 (0.254,0.492)	LMG	1.7074	2.0178	65	38.1	66
Minimum	0.327 (0.213,0.439)	MLG	0.609	0.674	66.7	40	50
Median	0.335 (0.221,0.470)	LMG	0.791	1.0184	35	52.4	78
Normal Mean	0.157 (0.071,0.243)	LGM	0.5035	0.5969	35	38	47.6
Standard deviation	0.281 (0.162,0.401)	LGM	0.1155	0.1484	65	36	42.9
Third moment	0.204 (0.128,0.281)	GML	0.0009	0.0017	42	38.1	50
Uniformity	0.333 (0.207,0.442)	MLG	204.872	404.507	66.7	45	52
Entropy	0.290 (0.189,0.411)	LGM	6.3596	6.5006	60	24	66.7
Kurtosis	0.291 (0.168,0.413)	MGL	3.2049	4.0991	52.4	40	60
25 Percentile	0.174 (0.083,0.264)	MGL	0.3803	0.497	23.8	44	50
75 Percentile	0.194 (0.099,0.290)	LGM	0.5734	0.6748	35	32	61.9
95 Percentile	0.221 (0.132,0.310)	GLM	0.7809	0.826	42.9	35	61.9

Abbreviations: L, Lymphoma; G, GBM; M, Metastatic; VUS, Volume Under the ROC Surface

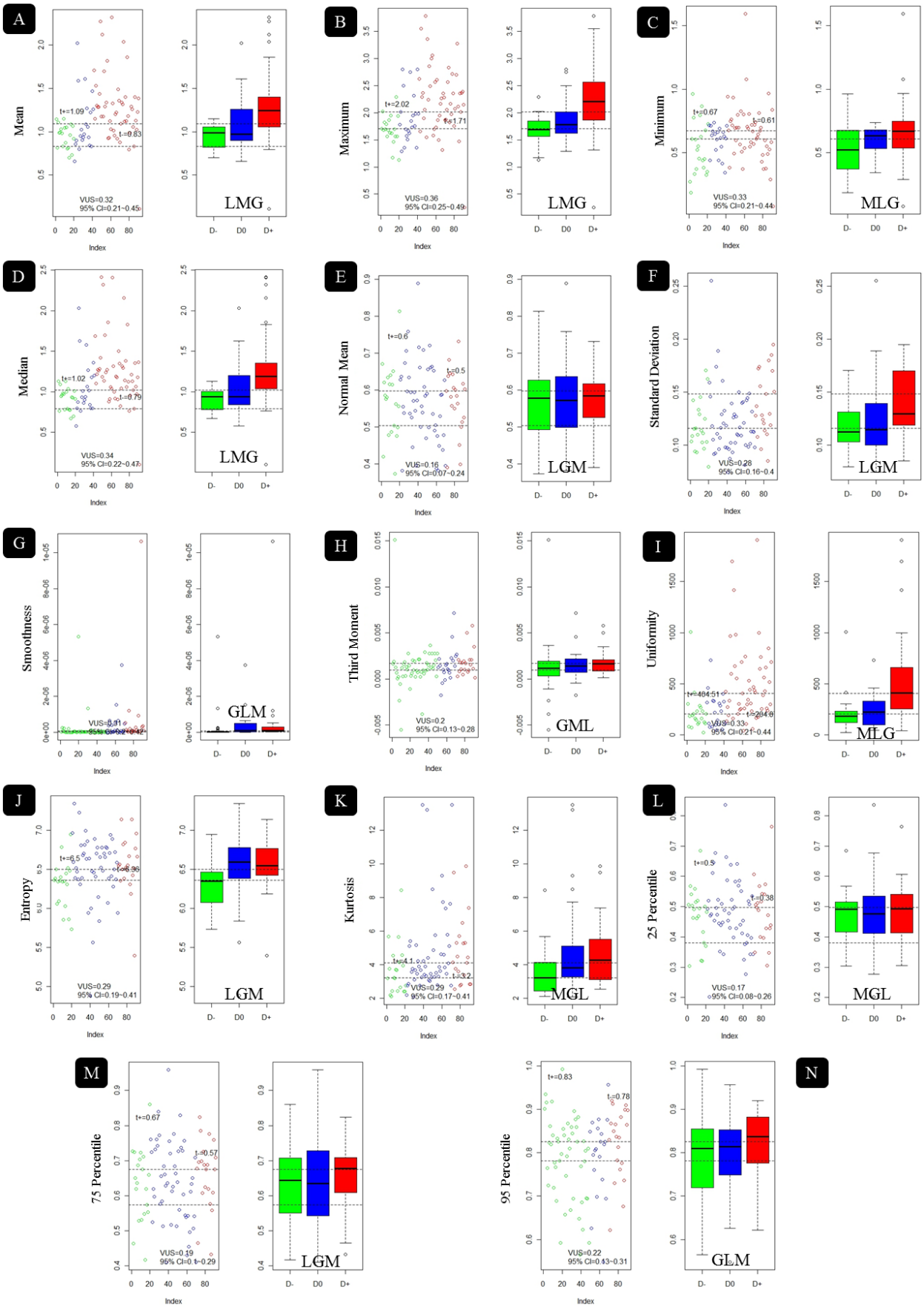

Figure 2. Continued; VUS of FOH features in Contrast-Enhanced MRIs (T1W); the box-plots and scatter-plots show the comparison of three investigated groups (in three-dimensional ROC). The order of plots is according to column 3 of Table 5; the order is shown in box-plot histograms.

Table 6 represented the VUS values of FOHs obtained from MRIs of peritumoral edematous regions. The VUS values of some FOHs in this table were better than the tumoral and contrast-enhanced region; albeit, in other cases, the worst results than the tumoral and contrast-enhanced region were seen. The best results belong to 25 Percentile with the VUS= 0.470 (0.312 to 0.617) for differentiation of LYM from MTT with CCR1= 70%, LYM from GMB with CCR2= 64%, and MTT from GBM with CCR3= 59.3%, however, when appalling the cut-offs 0.5352 and 0.675. Other potent results were obtained for the FOHs Standard deviation and Normal Mean. The weakest result was for VUS of ADC-Maximum equal to 0.168 (0.083 to 0.251) when cut-off 2.0135 and 2.2847 were used to differentiate LYM from GBM (CCR1= 50%), LYM from MTT (CCR2= 40.7%), and GBM from MTT (CCR3= 28%) (Table 6). Figure 3, represented the VUS scatter-plot and box-plots of each FOH feature for the peritumoral edematous regions MRIs.

Table 6. VUS values and related cut-off points for each FOH feature extracted from MRIs of EDEM category.

FOH features	VUS (95% CI)	Ordered Categories	Cut 1	Cut 2	CCR_1%	CCR_2%	CCR_3%
Mean	0.314 (0.2,0.433)	LMG	1.1573	1.4379	55	44	62.9
Maximum	0.168 (0.083,0.251)	LGM	2.0135	2.2847	50	40.7	28
Minimum	0.306 (0.175,0.448)	MLG	0.5172	0.759	36	55	62.9
Median	0.31 (0.180,0.419)	LGM	1.2779	1.6632	70	74.1	24
Normal Mean	0.458 (0.304,0.593)	LGM	0.6389	0.7345	75	64	59.3
Standard deviation	0.464 (0.318,0.618)	GLM	0.1149	0.1305	81.5	50	60
Third moment	0.402 (0.258,0.556)	GML	0.0009	0	44	59.3	85
Uniformity	0.204 (0.110,0.320)	MLG	713.9367	1990.376	32	50	59.3
Entropy	0.355 (0.233,0.476)	GLM	6.5275	6.813	51.9	55	52
Kurtosis	0.187 (0.101,0.289)	MLG	2.6594	3.1256	40	25	62.9
25 Percentile	0.470 (0.312,0.617)	LMG	0.5352	0.675	70	64	59.3
75 Percentile	0.326 (0.211,0.448)	LMG	0.708	0.8322	70	52	37
95 Percentile	0.301 (0.182,0.408)	LMG	0.8089	0.927	65	68	29.6

Abbreviations: L, Lymphoma; G, GBM; M, Metastatic; VUS, Volume Under the ROC Surface.

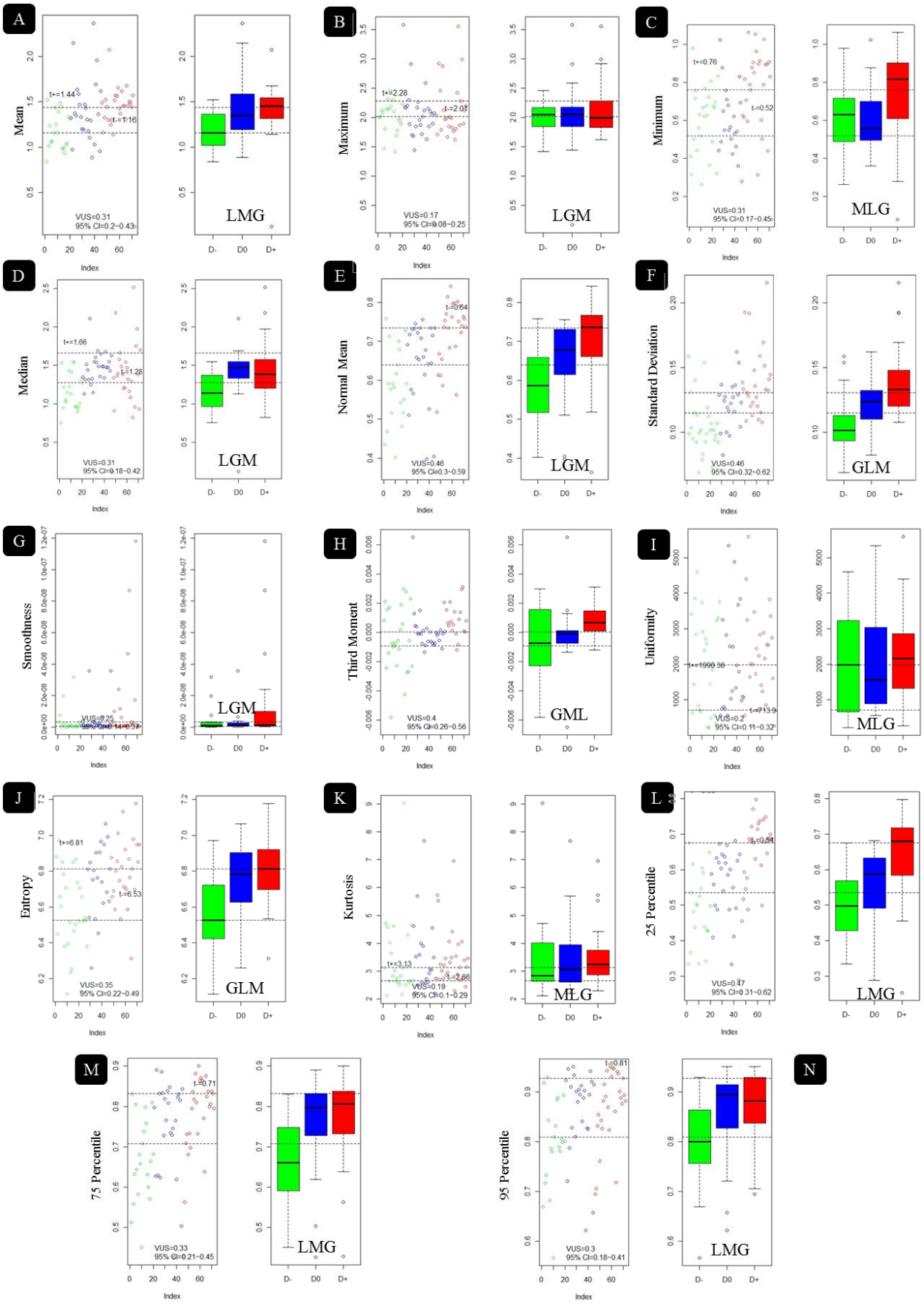

Figure 3. VUS of FOH features in MRIs from peritumoral edematous regions (EDEM group); the box plots and scatter plots show the comparison of three investigated groups (in three-dimensional ROC). The order of plots is according to column 3 of Table 6; the order is shown in box-plot histograms.

Figures 4 to 9 showed the two dimensional ROC curves of FOH features that were plotted using GBM and MTT or MTT and LYM groups data according to the tumor, contrast-enhanced, and peritumoral edematous regions MRIs. ROC curves of tumoral region MRIs that were plotted according to the GBM and MTT tumors have no significant results except in Uniformity, Smoothness, and 95 Percentile (Figure 4; the images with P-values< 0.05).

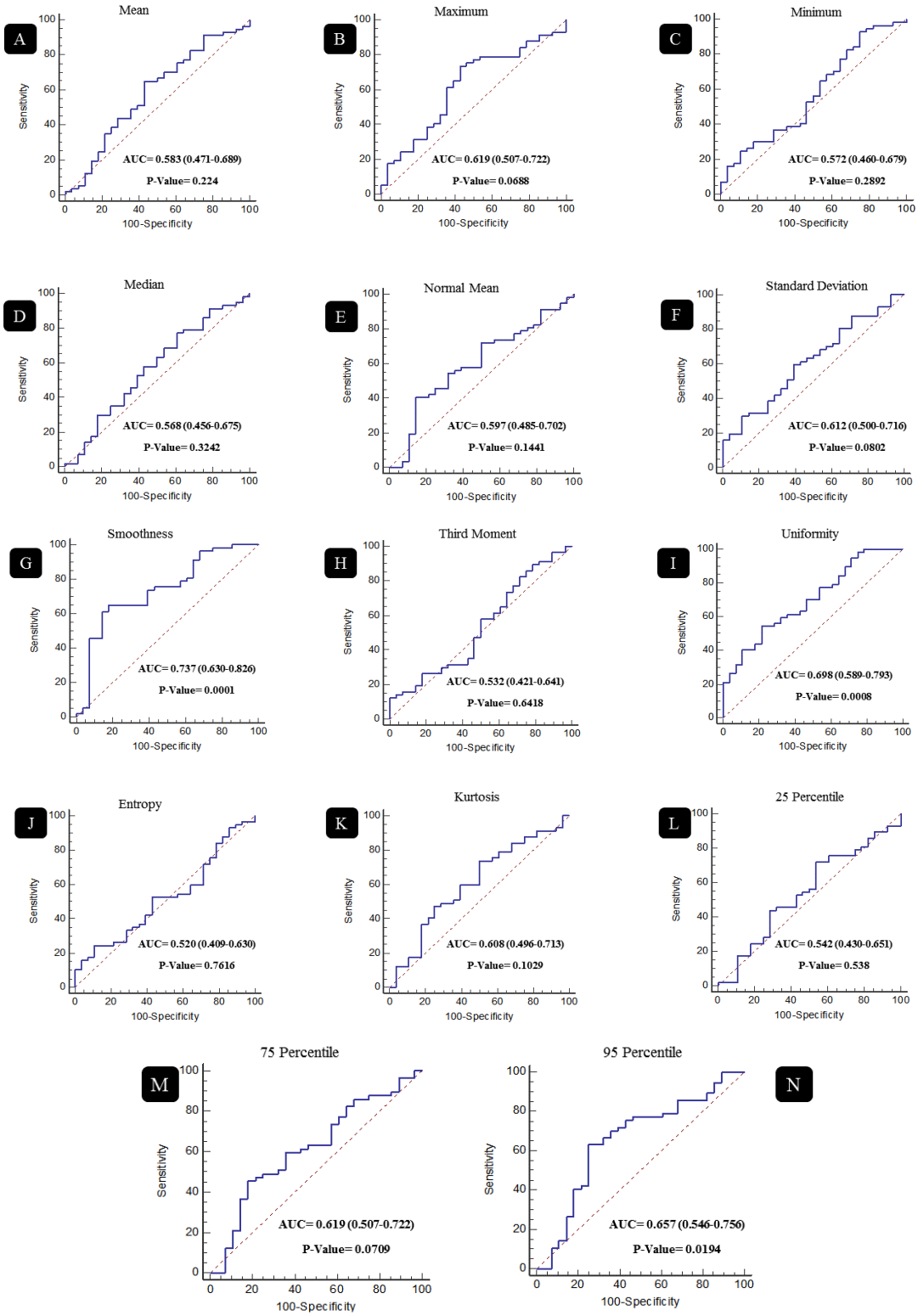

Figure 4. ROC curves of FOH features obtained from flair MRIs and show the power of each ADC statistic in the differential diagnosis between GBM and Metastatic tumors. The area under the curve (AUC) (95% level for AUC) and P-values are shown for each image.

Figure 5 showed the ROC curves of tumoral region MRIs of MTT and LYM; there were no significant results except in Normal Mean, Smoothness, Kurtosis, 75 and 95 Percentiles (Figure 5; the images with P-values< 0.05).

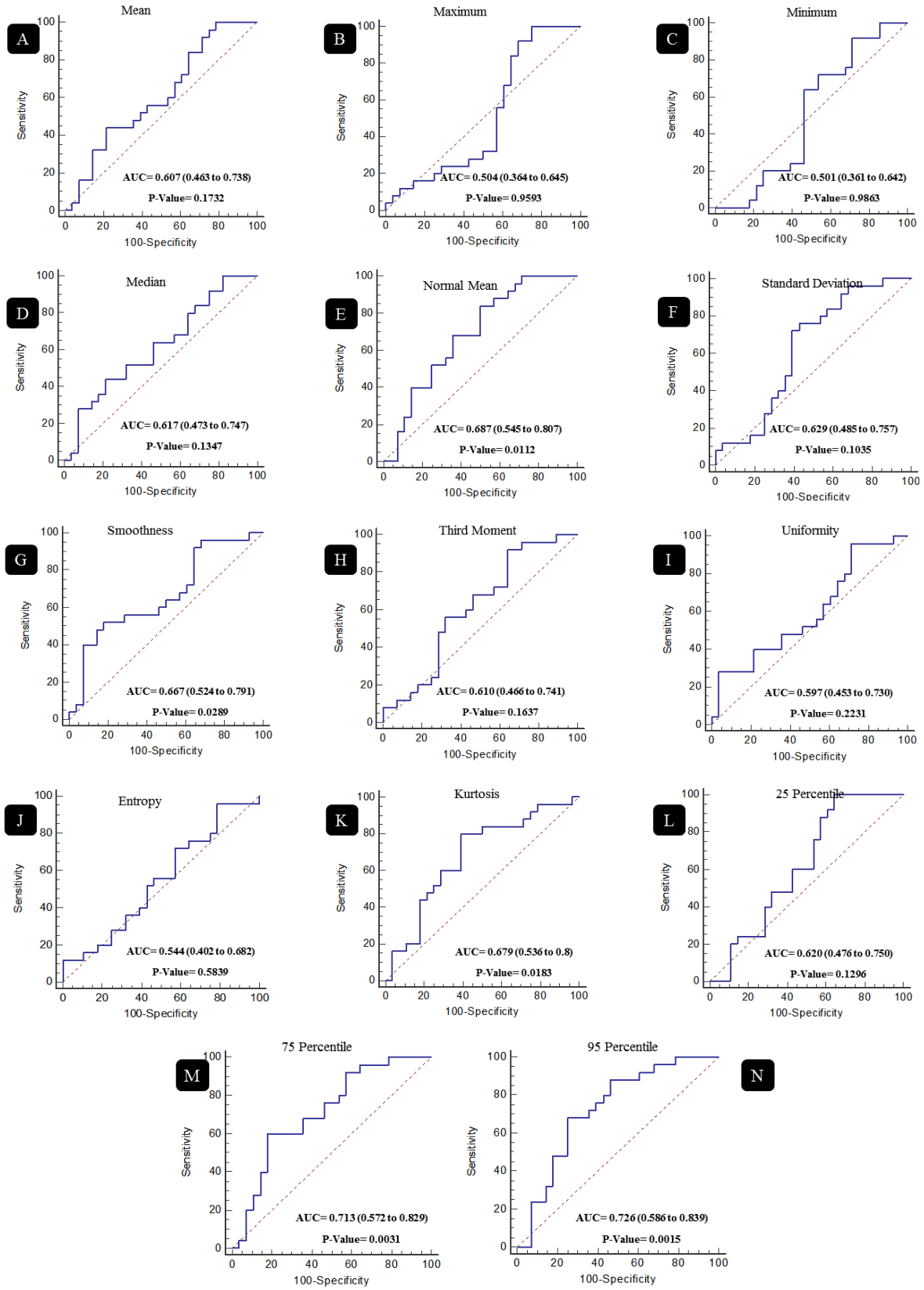

Figure 5. ROC curves of FOH features obtained from flair MRIs and show the power of each ADC statistic in the differential diagnosis between Metastatic tumors and Lymphoma. The area under the curve (AUC) (95% level for AUC) and P-values are shown for each image.

Figure 6 showed the two-dimensional ROC curves of contrast-enhanced MRIs plotted using GBM and MTT data. The significant results including mean, maximum, minimum, median, Normal Mean, and Standard deviation, Smoothness, Uniformity, and Kurtosis (Figure 6; the images with P-values < 0.05).

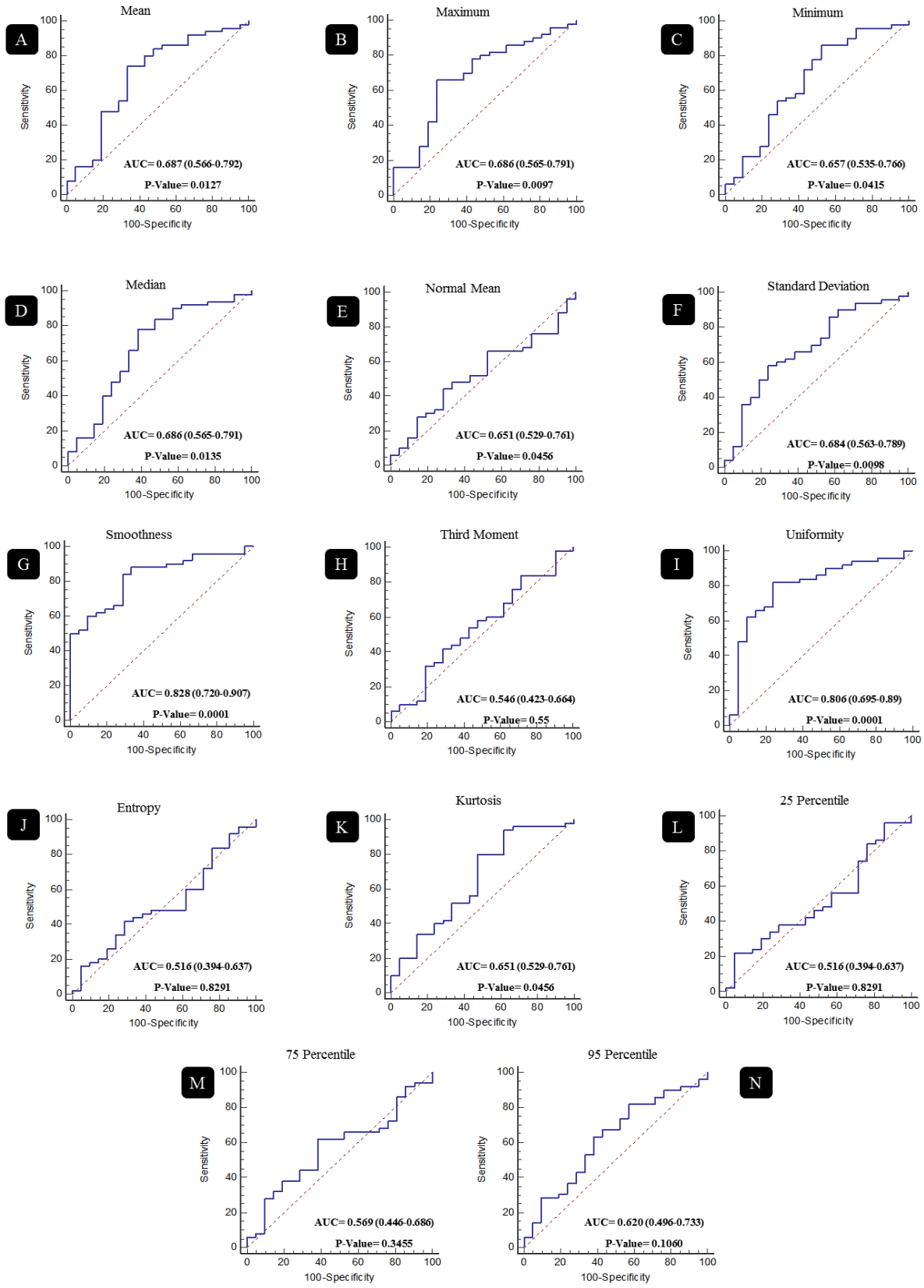

Figure 6. ROC curves of FOH features obtained from contrast-enhanced MRIs and show the power of each ADC statistic in the differential diagnosis between GBM and Metastatic tumors. The area under the curve (AUC) (95% level for AUC) and P-values are shown for each image.

Figure 7 showed the ROC curves of contrast-enhanced MRIs plotted by MTT and LYM groups ADC values. Except for the Standard deviation, Entropy, and Kurtosis (Figure 7; the images with P-values < 0.05), other AUCs do have not high values to that to be meaningful for differentiation of MTT from LYM lesions.

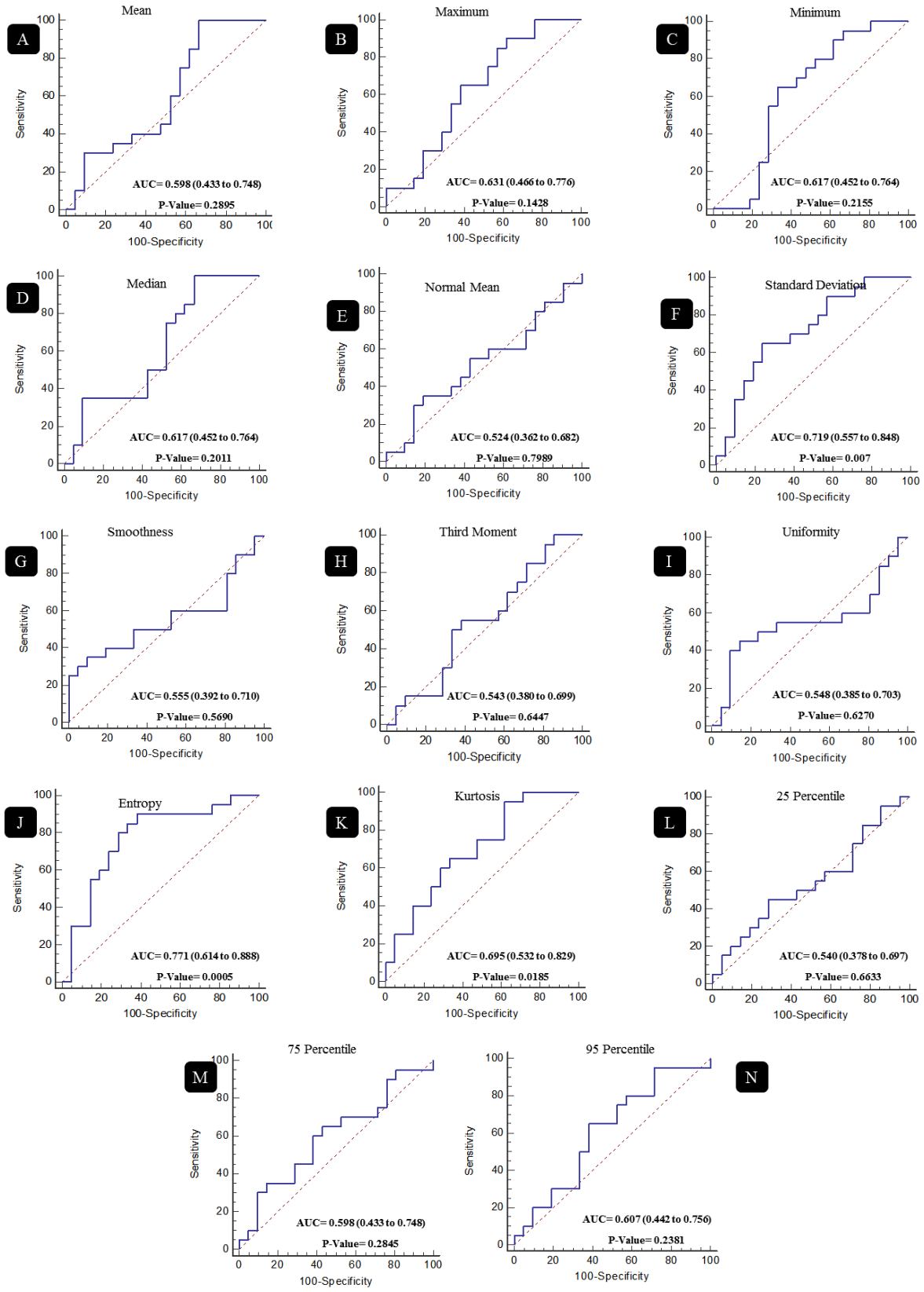

Figure 7. ROC curves of FOH features obtained from contrast-enhanced MRIs and show the power of each ADC statistic in the differential diagnosis between Metastatic tumors and Lymphoma. The area under the curve (AUC) (95% level for AUC) and P-values are shown for each image.

Figure 8 showed the ROC curves of peritumoral edematous regions MRIs plotted according to the ADC values of GBM and MTT data. The meaningful AUCs that could be applicable in decision making include the Minimum, Normal Mean, Standard deviation, Entropy, and 25 Percentile (Figure 8; the images with P-values < 0.05).

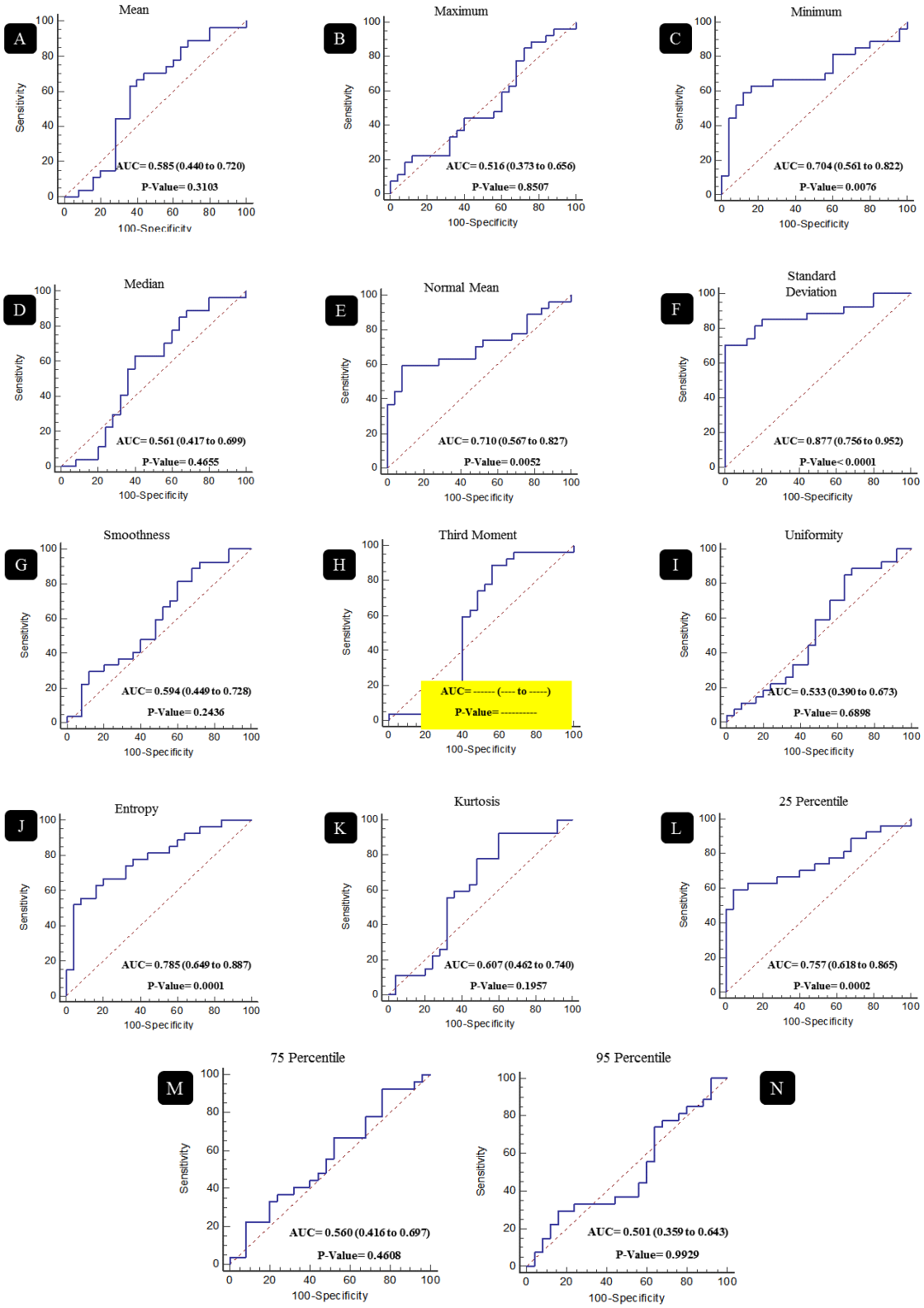

Figure 8. ROC curves of FOH features obtained from peritumoral edematous regions MRIs and show the power of each ADC statistic in the differential diagnosis between GBM and Metastatic tumors. The area under the curve (AUC) (95% level for AUC) and P-values are shown for each image.

Figure 9 shows the ROC curves of peritumoral edematous regions MRIs plotted according to the ADC values of MTT and LYM data. The meaningful results include the Mean, Median, Normal Mean, Standard deviation, Third moment, 25, 75, and 95 Percentiles (Figure 9; the images with P-values < 0.05).

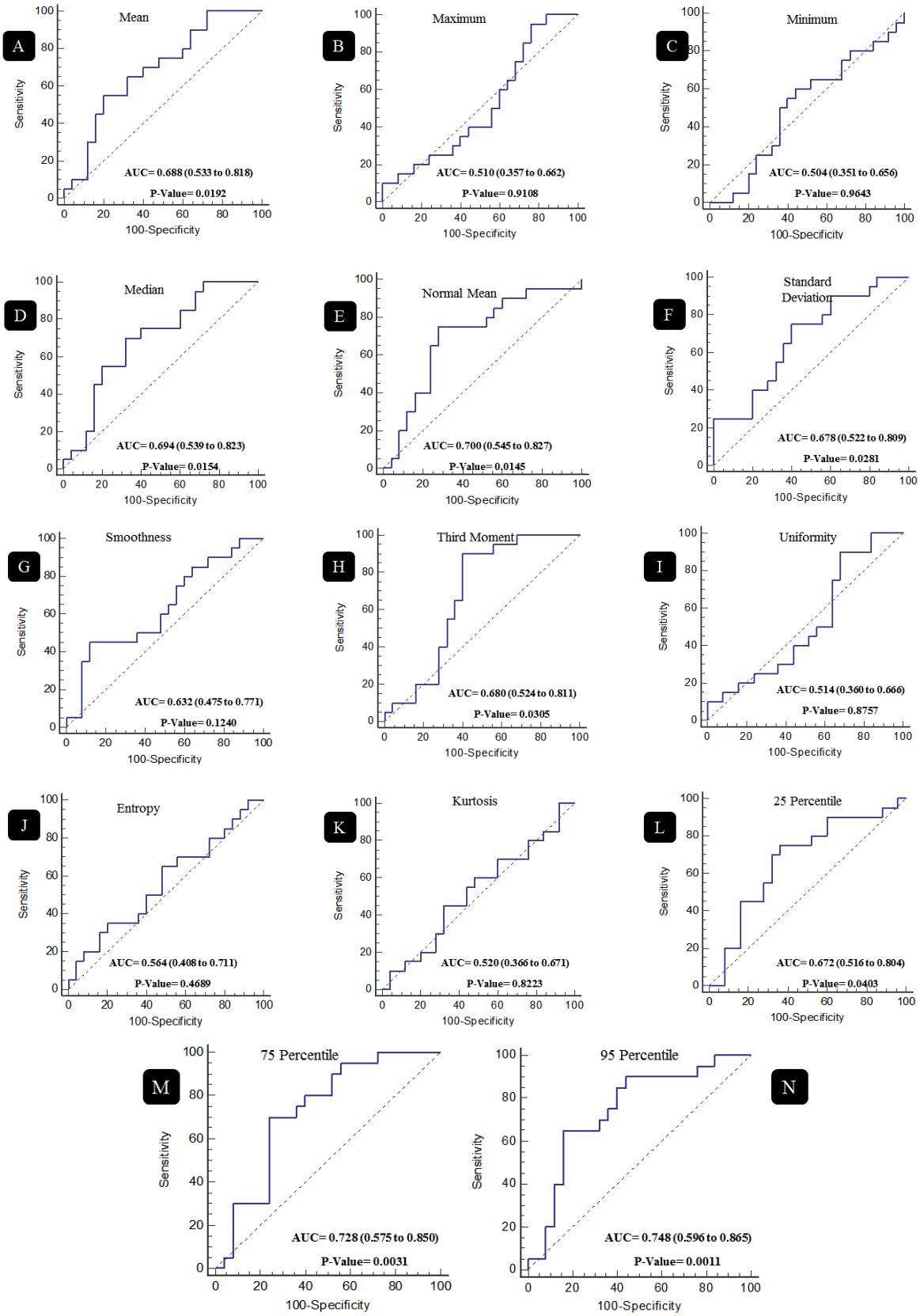

Figure 9. ROC curves of FOH features obtained from peritumoral edematous regions MRIs and show the power of each ADC statistic in the differential diagnosis between Metastatic tumors and Lymphoma. The area under the curve (AUC) (95% level for AUC) and P-values are shown for each image.

Discussion

Glioblastoma is the most prevalent brain tumor that its differentiation from other types of malignancies is essential [11] and problematic for neurologists and neurosurgeons before invasive operation. The problem is more complicated clinically when the metastasis of malignancies be present. CNS lymphomas could be primary and secondary in their types. Differential diagnosis of CNS lymphomas from other types of tumors is a need in diagnostic radiology [8].

Surgical pathology methods for differential diagnosis of brain tumors are applicable post-operation whereas radiologic methods are less invasive with repeatability because of their entities of safe to be done. Further, MRI-based diagnostic methods need not biopsy specimens and keep the patients away from erroneous extra-excision sampling methods [14]. On other hand, radiologic methods of diagnosis have their limitations especially because of similarities of shapes, maps, and the views obtained from each taken image of brain lesion [18]; furthermore, image analysis software and the radiology professionalist who select the ROIs and interpret the results to have a pivotal role in this area. MRI modality is one of the helpful tools when FOH statistics were used for differential diagnosis[19]. MRI modalities also have been of choice in distinguishing primary from secondary CNS lymphoma and have been preferred over computerized tomography (CT) scan techniques [8].

Comparative results showed that first-order histogram statistics obtained from ADC maps are meaningfully different between the three types of brain malignancies investigated in the current report. Further, although most are in one direction, however, the Mean±SD value of each FOH statistic could be higher or lower than its value in another type of imaging protocol (Tumor, Contrast-Enhanced or Edematous); e.g. the Standard deviation of Contrast-enhanced MRIs of GBM was higher than LYM whereas in the peritumoral edematous MRIs LYM lesions had higher values than GBM. We think that such algorithms may be critical in making a decision map when interpreting the results of FOH features of MRIs. **Table7** shows the order of significant ADC values using three different ROI including Tumor, Contrast-Enhanced, and Peritumoral Edematous Regions. The orders propose which tumor has higher values when comparative evaluation of FOHs is done; then, which type of malignancy is more probable.

Table 7. Order of significant ADC (Mean±SD) values using three different MR imaging methods including Tumor, Contrast-Enhanced and Peritumoral Edematous Regions. The orders propose that which tumor has higher values when comparative evaluation of FOHs is performs; then, which type of malignancy is more probable.

MR Imaging Protocol	FOHs	Order of significant Values
Tumor regions	Minimum	GBM>LYM>MTT
	75 Percentile	MTT>GBM>LYM
	95 Percentile	GBM > MTT >LYM
Contrast-Enhanced	Mean	GBM>MTT>LYM
	Maximum	GBM>MTT>LYM
	Median	GBM>MTT>LYM
	Minimum	GBM>LYM>MTT
	Uniformity	GBM>LYM>MTT
	Entropy	MTT>GBM>LYM
Peritumoral Edematous Regions	Mean	GBM>MTT>LYM
	Median	MTT>GBM>LYM
	Normal Mean	MTT > GBM >LYM
	Standard deviation	MTT>LYM>GBM
	Third moment	LYM >MTT> GBM
	Entropy	MTT>LYM>GBM
	25 Percentile	GBM>MTT>LYM
	75 Percentile	GBM>MTT>LYM
	95 Percentile	GBM>MTT>LYM

In the current study, we used the VUS analysis to evaluate two cut-off points in each case of the MR imaging method and for differential diagnosis of GBM, LYM, and MTT. Further, and using VUS, the correct classification rates were determined and proposed for each differential diagnosis among three classes of tumors. Cut-offs of FOH features, using VUS analysis could be considered in clinical practices with proper correction rates. The correct diagnosis is important for critical appraisal, decision making, and treatment planning especially for neuro-radiologists, neurologists, and neurosurgeons.

Two dimensional ROC curves had only a few significant estimations than VUS analysis if we consider the P-values of ROCs and the critical decision-point of 0.17 for three-dimensional ROC (VUS). Two-way ROCs showed us the most important FOHs for differential diagnosis of two groups of malignancies whereas VUS showed the correct classification rate of FOHs when three separate types of malignancies were probable.

Toh et al. used Fractional Anisotropy (FA) and ADC values for differential diagnosis of primary brain LYM from GBM; they, have reported that brain LYM had significantly lower ADCs and FA values than GBM tumors [7]. Toh et al. reported about ADC values agree with our findings. In the present research, most FOH features of the LYM lesions had lower values than GBM and MTT tumors when ROI was taken in a Tumor or contrast-enhanced manner or from peritumoral edematous regions. However, in the current report, we proposed two cut-off points and their CCR% which reduce the uncertainty of diagnosis. We think, using the proposed cut-offs for each FOH feature, clinical radiologists could interpret and make more certain reports for neurosurgeons and neurologists before starting operation planning or therapeutic regimens.

Lu et al. used mean diffusivity and FA for differentiation of GBM and the meningioma-metastasis tumors. They compared the ROI of tumoral lesions and peritumoral edematous regions MRIs and have shown that MDs were significantly different between GBM and meningioma-metastasis tumors [20]. The results of the current study confirmed Lu et. al. findings. For example, that is applicable for other findings of our study, using cut-offs represented in **Table 6**, especially that of 25 Percentile (Cut-off1= 0.5352; Cut-off2= 0.677; VUS=0.470), LYM lesions would be distinguished from MTTs with at least 70% CCR; LYM would be distinguished from GBMs in at least 64% CCR, and MTTs would be diagnosed from GBM in 59.2% of cases when MRIs was taken from peritumoral edematous regions.

Calli et al. evaluated 48 patients with brain tumors and have seen that ADCMinimum values were statistically different between LYM and astrocytoma but not between LYM and metastatic lesions, and between GBM, astrocytoma, and MTTs. They proposed the ADC statistics as the right tools for the differentiation of common CNS tumors using contrast-enhanced MRIs [18]. In addition, Chen et al. stated the ADCMinimum importance for the prediction of neuroepithelial tumor grading where this value distinguishes the high and low grades of gliomas [21]. Calli et al. [18] and Chen et al. [21] have not proposed any cut-off value for differentiation of the mentioned tumors; anyway, we have shown that ADC statistics may have contained cut-off points for differentiation among GBM, LYM, and MTTs and the VUS results differentiate the usability of our work from other published papers in this field of research.

However, the ADC statistics that we have investigated are not limited to the $ADC_{Minimum}$ and other statistics were also studied. **Tables 1-3** and **Figures 4-9** contain the comparative statistics for FOH features and two-dimensional ROC curves, respectively. As mentioned in results any type of imaging protocol had some significant P-values. Then, we think that other investigators should consider the evaluations of the FOH feature sets that we have, in the current study; however, if more significant aspects need to be used in distinguishing the tumor types.

In the present report, we have shown that VUS statistics may be as proper biomarkers when distinguishing of more than two types of lesions is of interest. We think that our report is the first one in its type and should be considered as a primary report that its results need to be re-evaluated by other investigators in the field. We have seen that although two-dimensional ROC curves calculate the AUCs when comparing the ADC values of two different types of tumor and this is helpful in distinguishing them from each other, anyway, VUS analysis adds another capability to the ROCs; VUS proposed that how we can categorize the tumor types with the most probable and largest CCR value.

As mentioned previously, most studies focused on the $ADC_{Minimum}$ values when evaluating the differential diagnostic role of FOHs. Lee et al., also showed that the importance and usability of $ADC_{Minimum}$ in the differentiation of "Glioblastoma (GBM) from solitary metastatic lesions". In the Lee et al. study the $ADC_{Minimum}$ was 1.152 ± 0.29 in GBM and was 1.145 ± 0.25 in MTT lesions; these two regions were not significantly different statistically. However, in the peritumoral regions of GBM and MTTs, Lee et al. reported significantly different values ($ADC_{Minimum}$ for GBM = 1.466 ± 0.24 and MTT= 1.829 ± 0.25). Further, they proposed to determine that the cut-off value= 1.302 × 10−3 mm2/s for $ADC_{Minimum}$, had proper sensitivity (82.9%) and specificity (78.9%) for differential diagnosis of GBM tumors from MTTs [22]. Compared to Lee et al. study, we showed that $ADC_{Minimum}$ is significantly different among GBM, LYM and MTTs in peritumoral regions MRIs (**Table 3**). However, other ROI types, Tumor and Contrast-Enhanced, had not shown significant $ADC_{Minimum}$ values among the three types of lesions. On other hand, with a brief review on **Tables 1-3**, it is obvious that other FOH statistics such as ADC_{Mean}, $ADC_{Maximum}$, ADC_{Median}, $ADC_{Smoothness}$, $ADC_{Uniformity}$, $ADC_{75\ Percentile}$ and $ADC_{95\ Percentile}$ (**Table 1**; Flair MRIs) were meaningfully different among GBM, LYM, and MTTs. Furthermore, in the Contrast-Enhanced MRIs ADC_{Mean}, $ADC_{Maximum}$, ADC_{Median}, $ADC_{Standard\ deviation}$, $ADC_{Uniformity}$, and $ADC_{Entropy}$ were significantly different between GBM, LYM, and MTTs. As **Table 3** showed and we mentioned previously, in addition to the $ADC_{Minimum}$, other FOHs including ADC_{Mean}, ADC_{Median}, $ADC_{Normal\ Mean}$, $ADC_{Standard\ deviation}$, $ADC_{Third\ moment}$, $ADC_{Entropy}$,

$ADC_{25\ Percentile}$, $ADC_{75\ Percentile}$ and $ADC_{95\ Percentile}$ were different significantly among GBM, LYM and MTTs when MRIs of peritumoral edematous regions explored in the current investigation. All these mentioned evidence emphasize the usability of other FOHs in addition to the $ADC_{Minimum}$ for differential diagnosis of GBM, LYM, MTT, or other types of brain tumors. Furthermore, in the present study, we used a different type of analysis that is lesser under attention in clinical investigations. VUS analysis is not previously used for determining the Cut-Off points of ADC values when evaluating differential diagnosis application of MRIs; at least our searches had not any result.

In conclusion, it is proposed that the Cut-Off points represented in the current study we evaluated in clinical settings and by the clinical radiologists, neurologists, and neurosurgeons before starting to interpret, treatment, and operation, respectively. Using the two Cut-Off points, helps these specialists to make a better performance and decision when differentiating brain tumors with a high grade of correct classification rate (CCR) and concurrently. It is emphasized that as the results of this study are novel because of the usage of VUS analysis, then confirmatory studies are needed by other investigators. We suggest that future studies be the focus, in addition to the GBM, LYM, and MTT, on the differentiation of other types of brain tumors such as GBM with oligodendroglial components, astrocytic tumors, oligoastrocytoma tumors, neuroepithelial tumors, and ependymal tumors. Then, the horizons of the field are so wide that many investigators can design and perform valuable studies. Certainly, the results of such surveys will be helpful in the prevention of unfavorable diagnostic methods when manipulating the brain via surgical pathology performances. Furthermore, it is possible that Cut-Off points obtained from VUS analysis to be valuable in the monitoring of chemotherapies, in addition to differential diagnosis.

Highlights

What Is Already Known?
ADC statistics can be valuable in distinguishing three types of brain tumors.

What Does This Study Add?
VUS analysis is a useful method for categorizing types of brain tumors. Using the application of FOHs and proposed cut-off points for them by the VUS analysis, the differentiation of more than two types of brain tumors would be possible, concurrently.

Authors' Contributions
Concepts: Mersad Mehrnahad, Morteza Sanei Taheri, Farnaz Kimia, Hamidreza Saligheh Rad, Robabeh Ghodssi Ghassem Abadi.Data gathering: Mersad Mehrnahad, Morteza Sanei Taheri, Farnaz Kimia, Hamidreza Saligheh Rad, Robabeh Ghodssi Ghassem Abadi. Writing and editing the paper: SMersad Mehrnahad, Morteza Sanei Taheri, Farnaz Kimia, Hamidreza Saligheh Rad, Robabeh Ghodssi Ghassem Abadi.

Acknowledgements
None

Conflicts of Interest Disclosures
We declare there was no conflict of interest.

Consent for Publication
We declare consent for publication.

Ethics approval
Ethical committee of Shahid Beheshti University of Medical Sciences confirmed the protocol of this study.

Funding/Support
None

References

1. Ceschin R, Kurland BF, Abberbock SR, et al. Parametric Response Mapping of Apparent Diffusion Coefficient as an Imaging Biomarker to Distinguish Pseudoprogression from True Tumor Progression in Peptide-Based Vaccine Therapy for Pediatric Diffuse Intrinsic Pontine Glioma. *AJNR American journal of neuroradiology* 2015; **36**(11): 2170-6. doi: 10.3174/ajnr.A4428

2. Poretti A, Meoded A, Cohen KJ, Grotzer MA, Boltshauser E, Huisman TA. Apparent diffusion coefficient of pediatric cerebellar tumors: a biomarker of tumor grade? *Pediatr Blood Cancer* 2013; **60**(12): 2036-41, doi: 10.1002/pbc.24578.

3. Shin HJ, Kim SH, Lee HJ, et al. Tumor apparent diffusion coefficient as an imaging biomarker to predict tumor aggressiveness in patients with estrogen-receptor-positive breast cancer. *NMR Biomed* 2016; **29**(8): 1070-8, doi: 10.1002/nbm.3571.

4. Cui Y, Zhang XP, Sun YS, Tang L, Shen L. Apparent diffusion coefficient: potential imaging biomarker for prediction and early detection of response to chemotherapy in hepatic metastases. *Radiology* 2008; **248**(3): 894-900, doi: 10.1148/radiol.2483071407.

5. Goryaynov SA, Potapov AA, Ignatenko MA, et al. [Glioblastoma metastases: a literature review and a description of six clinical observations]. *Zh Vopr Neirokhir Im N N Burdenko* 2015; **79**(2): 33-43, doi: 10.17116/neiro201579233-43.

6. Doskaliyev A, Yamasaki F, Ohtaki M, et al. Lymphomas and glioblastomas: differences in the apparent diffusion coefficient evaluated with high b-value diffusion-weighted magnetic resonance imaging at 3T. *European journal of radiology* 2012; **81**(2): 339-44, doi: 10.1016/j.ejrad.2010.11.005.

7. Toh CH, Castillo M, Wong AM, et al. Primary cerebral lymphoma and glioblastoma multiforme: differences in diffusion characteristics evaluated with diffusion tensor imaging. *AJNR American journal of neuroradiology* 2008; **29**(3): 471-5, doi: 10.3174/ajnr.A0872.

8. Haldorsen IS, Espeland A, Larsson EM. Central nervous system lymphoma: characteristic findings on traditional and advanced imaging. *AJNR American journal of neuroradiology* 2011; **32**(6): 984-92, doi: 10.3174/ajnr.A2171.

9. Jakubovic R, Zhou S, Heyn C, et al. The predictive capacity of apparent diffusion coefficient (ADC) in response assessment of brain metastases following radiation. *Clin Exp Metastasis* 2016; **33**(3): 277-84, doi: 10.1007/s10585-016-9778-x.

10. Miquelini LA, Perez Akly MS, Funes JA, Besada CH. Usefulness of the apparent diffusion coefficient for the evaluation of the white matter to differentiate between glioblastoma and brain metastases. *Radiologia* 2016; **58**(3): 207-13, doi: 10.1016/j.rx.2015.10.004.

11. He J, Mokhtari K, Sanson M, et al. Glioblastomas with an oligodendroglial component: a pathological and molecular study. *Journal of Neuropathology & Experimental Neurology* 2001; **60**(9): 863-71, doi: 10.1093/jnen/60.9.863.

12. Sutherland-Smith J, King R, Faissler D, Ruthazer R, Sato A. Magnetic resonance imaging apparent diffusion coefficients for histologically confirmed intracranial lesions in dogs. *Veterinary radiology & ultrasound : the official journal of the American College of Veterinary Radiology and the International Veterinary Radiology Association* 2011; **52**(2): 142-8, doi: 10.1111/j.1740-8261.2010.01764.x.

13. Chen L, Liu M, Bao J, et al. The correlation between apparent diffusion coefficient and tumor cellularity in patients: a meta-analysis. *PloS one* 2013; **8**(11): e79008, doi: 10.1371/journal.pone.0079008.

14. Khayal IS, VandenBerg SR, Smith KJ, et al. MRI apparent diffusion coefficient reflects histopathologic subtype, axonal disruption, and tumor fraction in diffuse-type grade II gliomas. *Neuro-oncology* 2011; **13**(11): 1192-201, doi: 10.1093/neuonc/nor122.

15. He X, Frey EC. The meaning and use of the volume under a three-class ROC surface (VUS). *IEEE Trans Med Imaging* 2008; **27**(5): 577-88, doi: 10.1109/TMI.2007.908687.

16. Mossman D. Three-way ROCs. *Medical decision making: an international journal of the Society for Medical Decision Making* 1999; **19**(1): 78 , doi: 10.1177/0272989X9901900110.

17. Xiong C, van Belle G, Miller JP, Morris JC. Measuring and estimating diagnostic accuracy when there are three ordinal diagnostic groups. *Statistics in medicine* 2006; **25**(7): 1251-73, doi: 10.1002/sim.2433.

18. Calli C, Kitis O, Yunten N, Yurtseven T, Islekel S, Akalin T. Perfusion and diffusion MR imaging in enhancing malignant cerebral tumors. *European journal of radiology* 2006; **58**(3): 394-403, doi: 10.1016/j.ejrad.2005.12.032.

19. Aggarwal N, Agrawal R. First and second order statistics features for classification of magnetic resonance brain images. 2012, doi: 0.4236/jsip.2012.32019.

20. Lu S, Ahn D, Johnson G, Law M, Zagzag D, Grossman R. Diffusion-tensor MR imaging of intracranial neoplasia and associated peritumoral edema: introduction of the tumor infiltration index. *Radiology* 2004; **232**(1): 221-8, doi: 10.1148/radiol.2321030653.

21. Chen Z, Ma L, Lou X, Zhou Z. Diagnostic value of minimum apparent diffusion coefficient values in prediction of neuroepithelial tumor grading. *Journal of Magnetic Resonance Imaging* 2010; **31**(6): 1331-8, doi: 10.1002/jmri.22175.

22. Lee JH, Jung TY, Jung S, et al. Performance status during and after radiotherapy plus concomitant and adjuvant temozolomide in elderly patients with glioblastoma multiforme. *Journal of clinical neuroscience : official journal of the Neurosurgical Society of Australasia* 2013; **20**(4): 503-8, doi: 10.1016/j.jocn.2012.03.044.